applied sciences

MDPI

Article

Development of Energy Storage Systems for High Penetration of Renewable Energy Grids

Lun-Yi Lung [1], Tsan-Yu Chou [2], Wen-Ching Chang [1] and Cheng-Chien Kuo [1,*]

[1] Department of Electrical Engineering, National Taiwan University of Science and Technology, Taipei 106335, Taiwan; d11107004@mail.ntust.edu.tw (L.-Y.L.); d10907006@mail.ntust.edu.tw (W.-C.C.)
[2] Graduate Institute of Energy and Sustainability Technology, National Taiwan University of Science and Technology, Taipei 106335, Taiwan; d11253002@mail.ntust.edu.tw
* Correspondence: cckuo@mail.ntust.edu.tw; Tel.: +886-2-2733-3141 (ext. 7710)

Abstract: As the proportion of renewable energy generation systems increases, traditional power generation facilities begin to face challenges, such as reduced output power and having the power turned off. The challenges are causing changes in the structure of the power system. Renewable energy sources, mainly wind and solar energy cannot provide stable inertia and frequency regulation capability. Ultimately, the power system's emergency response capability to face an N-1 is reduced, which leads to a reduction in system stability. Therefore, the application technology of the battery energy storage system is used to support the impact of changes in the new power system structure. This paper designed control technologies based on the WECC second-generation generic model, namely, dynamic regulation, steady regulation, and virtual inertia regulation. The models and control strategies are verified on Taiwan's 2025 power system target conditions, which consider the expected capacities for battery energy storage systems, and renewable energy sources with different load and N-1 fault levels. According to the simulation results, the capabilities of the RoCoF limitation, frequency nadir, frequency recovery, and system oscillation regulation are evaluated in the proposed strategies. Finally, the analysis results can help power operators make informed decisions when selecting and deploying battery energy storage systems.

Keywords: renewable energy; battery energy storage system; high-proportion renewable energy; lower inertia; power stability; RoCoF; frequency nadir

check for updates

Citation: Lung, L.-Y.; Chou, T.-Y.; Chang, W.-C.; Kuo, C.-C. Development of Energy Storage Systems for High Penetration of Renewable Energy Grids. *Appl. Sci.* **2023**, *13*, 11978. https://doi.org/10.3390/app132111978

Academic Editor: Rossano Musca

Received: 2 October 2023
Revised: 30 October 2023
Accepted: 31 October 2023
Published: 2 November 2023

Copyright: © 2023 by the authors. Licensee MDPI, Basel, Switzerland. This article is an open access article distributed under the terms and conditions of the Creative Commons Attribution (CC BY) license (https://creativecommons.org/licenses/by/4.0/).

1. Introduction

As the penetration of renewable energy generation systems in power systems gradually increases, it has both positive and negative impacts on power systems. The positive impacts of renewable energy generation systems on power systems include reducing carbon emissions, reducing dependence on imported energy price volatility, and so on. The global focus on decarbonization has elevated it to a crucial policy objective, stimulating the growth of renewable energy in various countries [1]. In addition, renewable energy generation systems can be integrated into power systems in each region and use their generation in that region, which can reduce energy loss during long-distance transmission. However, high penetration of renewable energy also brings new challenges, becoming a new issue facing power systems. If the converter equipment does not provide a virtual inertia function, the renewable energy generation system cannot provide inertia to the power system [2]. Reference [3] discusses various inertia emulation and frequency control techniques for grid-connected wind energy conversion systems. Reference [4] discusses wind and solar generation plants and their contributions to inertia in terms of frequency control strategies. In the future, power systems need to be planned and operated in different ways to maintain a certain level of reliability. In the past, power systems were composed of thermal generators, hydropower generators, diesel generators, and a small number of solar

and wind power generation systems, many of which are based on large rotating machines that are of high inertia. In the future, power systems will be composed of a majority of solar and wind power generation systems, a small number of traditional generators, and battery energy storage systems which are mainly inverter-based resources and which have low inertia. Currently, renewable energy in Taiwan is dominated by solar and wind energy which are both affected by factors such as the time and season. Solar and wind power generation is intermittent, uncontrollable, and gives large short-term output fluctuations, which have a negative impact on the power system [5,6].

According to the above, future power systems with a large number of inverter-based resources have the following problems compared to traditional power systems: reduced system inertia, weakened frequency regulation capability, weakened regional reactive power regulation capability [7], and increased requirements for the rise/fall active power speed of traditional units. Renewable energy can also be applied in the islanding operation and fault recovery strategy of a distribution network [8]. Battery energy storage systems can be derived from many auxiliary services according to different control strategies, such as frequency regulation reserve, peak shaving and valley filling, smoothing of solar output power, load dispatch, islanding operation, reactive power compensation, and virtual inertia provision. In [9], by operating the battery energy storage system and implementing an adaptive primary frequency control strategy, the system frequency is adjusted by flexibly and rapidly controlling the charge and discharge capabilities of the battery energy storage system. An integrated control approach combines decentralized and cluster-based load control in McMahon et al. [10], which uses a battery energy storage system to determine the activation and deactivation of flexible load clusters based on frequency measurements. Reference [11] studies the smoothing quality of the solar output power with the help of battery energy storage system, using a couple of approaches, such as low pass filtering (LPF), moving average (MA) filtering, the Gaussian filter (GF) and the Saviztky–Golay (S-G) filter. Reference [12] introduces a technical approach for employing the battery energy storage system to achieve load balancing and reactive power compensation within distribution grids. In [13–15], these strategies are able to provide inertial support and ensure secure frequency dynamics in isolated microgrids by using battery energy storage systems. These are all control strategies that assist in power system operation, balance with generation and load, recover the system to steady state in an N-1 event, and improve the stability and resilience of the power system. In the transmission and distribution services, battery energy storage systems can strategically charge and discharge energy at different periods. This helps alleviate the pressure on the transmission and distribution systems feeder capacity caused by renewable energy generation systems. Therefore, the goal of alleviating transmission and distribution congestion and improving renewable energy utilization rates is introduced in [16,17]. Reference [18] introduces a coordinated control strategy to efficiently utilize energy, enhancing the minimum frequency level of the frequency nadir of the system by coordinating wind turbines with permanent magnetic synchronous generators and battery energy storage systems. In [19,20], a simulation of a power supply system for a weather station, which comprises solar panels, batteries, and inverters, was produced. This simulation resulted in an enhanced reliability of the power system.

According to the abovementioned literature, it is understood that battery energy storage systems operate with varying benefits in different power systems under different strategies. However, the current literature lacks a comprehensive comparative analysis of various strategies, making it difficult to compare the advantages and disadvantages of these strategies in detail with the same battery energy storage system specifications. Therefore, this paper focuses on the detailed modeling and design of frequency regulation strategies and virtual inertia strategies based on the WECC second-generation generic model. Subsequently, the simulation conditions are based on the actual equipment locations and capacities of Taiwan's 2025 power system. Finally, according to the proposed WECC second-generation generic model, the three different strategies are simulated in

transient using the software PSS/E. These three strategies include dynamic regulation, static regulation, and virtual inertia regulation. According to the simulation results, the capabilities of each strategy are analyzed.

The advantages and disadvantages of transmission-scale battery energy storage operating frequency regulation and virtual inertia regulation will help power operators expand the basis for the capacity of battery energy storage systems under different strategies. Next, this paper is divided into four sections. Section 2 introduces the frequency regulation technology, which includes dynamic regulation strategy, static regulation strategy, and virtual inertia strategy. The virtual inertia strategy compares three methods: virtual synchronous machine, swing equation emulation, and synchronverter. Section 3 shows the designs of frequency regulation strategies based on the WECC second-generation generic model. Section 4 shows the results of transient simulations, which consider the capacity of the battery energy storage system, the capacity of renewable energy devices, the load level, and the N-1 level under different strategies. Section 5 contains the conclusion of the paper.

2. Battery Energy Storage System (BESS) Frequency Regulation Technology

The existing application technologies for frequency regulation on the Taiwan power system include such as static regulation (sReg) and dynamic regulation (dReg), among others. The novel virtual inertia control strategy has not yet been implemented, but it has been proposed by many scholars. The three strategies have different response times, deadband ranges, frequency response functions, and frequency ranges. Next, the strategies are introduced.

2.1. Static Regulation

Static regulation control is a unidirectional frequency compensation strategy. If the battery energy storage system detects a grid frequency of less than 59.88 Hz, it should respond to the frequency drop within a few seconds. It actively adjusts the output power of the battery energy storage system to 100% within 10 s to instantly compensate for active power and maintain grid frequency stability [21]. When the grid frequency, then, increases to 59.98 Hz, the output power of the battery energy storage system should be reduced to 0%. As shown in Figure 1, the output power of the frequency operating curve for static regulation control is shown. The curve from point C to point A is the open curve, and the curve from point B to point D is the closed curve.

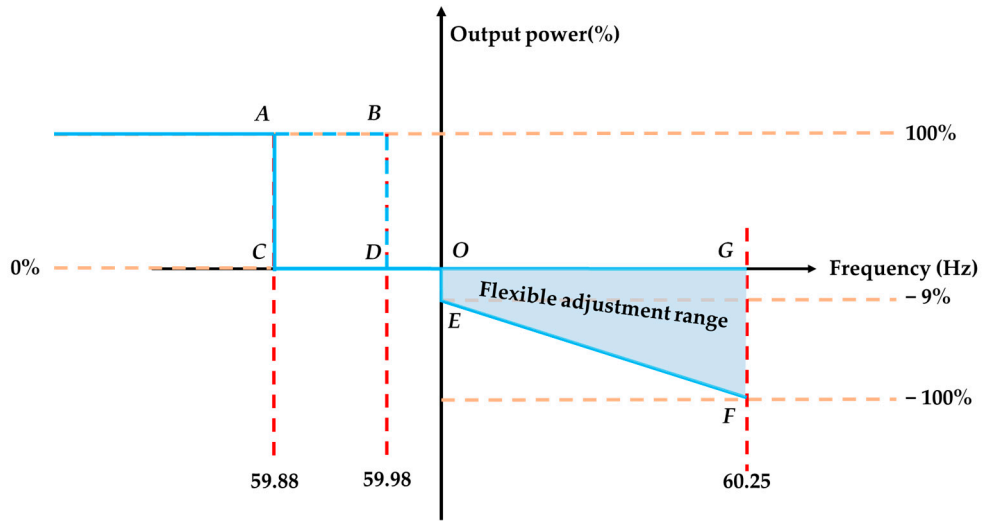


Figure 1. The frequency versus output power for static regulation control.

2.2. Dynamic Regulation

Dynamic regulation is a bidirectional frequency control strategy. The battery energy storage system actively adjusts its output power within 1 s based on the grid frequency

state, instantaneously compensating for active power to achieve grid frequency stability. As shown in Figure 2, the output power of the frequency operating curve for dynamic regulation control is shown. Dynamic regulation control has two types based on frequency control range, dReg 0.25 and dReg 0.50 [21]. The table of parameters for dReg 0.25 and dReg 0.5 are presented in Tables 1 and 2, respectively. The points in Figure 2 correspond to the corresponding symbols shown in Tables 1 and 2. In comparison, dReg 0.5 has a larger frequency operating range than dReg 0.25, indicating that dReg 0.25 has a larger parameter of droop gain.

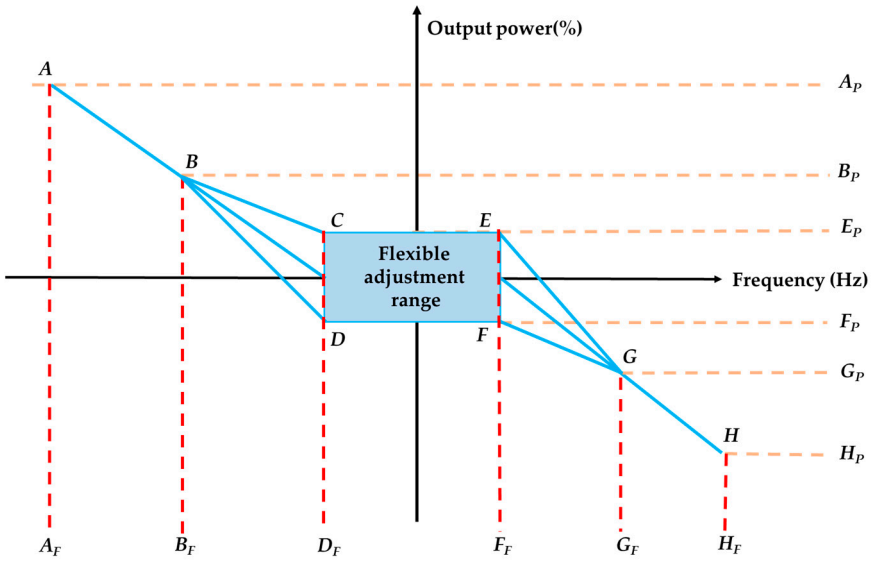


Figure 2. The frequency versus output power for dynamic regulation control.

Table 1. Parameter of dynamic regulation control @ dReg 0.25.

Symbol	Frequency (Hz)	Symbol	Power Ratio (%)
A_F	59.75	A_P	100
B_F	59.86	B_P	52
D_F	59.98	F_P~E_P	−9~9
F_F	60.02	F_P~E_P	−9~9
G_F	60.14	G_P	−52
H_F	60.25	H_P	−100

Table 2. Parameter of dynamic regulation control @ dReg 0.5.

Symbol	Frequency (Hz)	Symbol	Power Ratio (%)
A_F	59.50	A_P	100
B_F	59.75	B_P	48
D_F	59.98	F_P~E_P	−9~9
F_F	60.02	F_P~E_P	−9~9
G_F	60.25	G_P	−48
H_F	60.50	H_P	−100

2.3. Virtual Inertia Control

Virtual inertia control is a method that simulates the dynamic response of synchronous generators. It is also referred to as synchronous machine-based control. Common methods for virtual inertia control include a virtual synchronous machine, swing equation emulation, and synchronverter. The control approach of a virtual synchronous machine initially emulates the behavior of a synchronous generator, using power electronics to provide inertia effects. The control model of a virtual synchronous machine is based on the dq-axis

model of an electrically excited synchronous machine, considering electrical characteristics such as stator windings, rotor windings, excitation windings, and dampers. The DC side of the converter provides active power, while capacitors supply reactive power. The control logic of the virtual synchronous machine is implemented through digital signal processing control systems, which control the converter. Therefore, there is no physical mechanical component involved. Instead, a mathematical model within the controller outputs stable and dynamic responses of the virtual synchronous generator to simulate the response characteristics of a synchronous generator [22].

Swing equation emulation is developed based on the concept of a virtual synchronous machine and aims to address the challenge of distributed generation resources that are not able to provide inertia effects. The idea of this concept is to incorporate short-term energy storage devices like batteries, capacitors, and supercapacitors into distributed generation resources. By employing appropriate power electronic converter control mechanisms, it achieves the capability to provide virtual inertia. The scholar K. Visscher, leveraging the concept of a virtual synchronous machine, integrated the rotational kinetic energy equations into the control mechanisms of power electronic converters. This integration led to the derivation of virtual mechanical power equations, simulating the response of synchronous generators [23,24].

The control method of a synchronverter involves using the swing equations of a mechanical rotor to simulate the response characteristics of a synchronous generator. The electrical parameters of the synchronous generator are equivalently represented as part of the hardware circuit elements in the converter to provide virtual inertia. The impedance of the stator windings is equivalently represented as the inductance value of a filter, the phase voltage of the stator windings is equivalently represented as the voltage value of an output capacitor, and the back electromotive force generated by rotor movement is equivalently represented as the average voltage across switches. In the control system of a synchronverter, response parameters such as rotor inertia and damping constants are considered. Finally, control of the synchronverter is achieved through input variables such as the mechanical torque, rotor current, and mutual inductance between the rotor and stator [25].

Considering the components, dynamic characteristics, and control response parameters of the three methods mentioned, Table 3 lists the components and control parameters for the consideration of virtual inertia in these three approaches.

Table 3. Parameters of virtual inertia control method.

Control Method	Considered Components and Characteristics	Response Parameters
Virtual synchronous machine	Stator windings, rotor windings, excitation windings, damping	x
Swing equation emulation	X	Rotational inertia
Synchronverter	Stator winding impedance, stator winding phase voltage, rotor motion back EMF	Rotational inertia, damping constant

3. Frequency Regulation Technology Model

The WECC second-generation generic mode is adopted to design proposed control strategies in this section. The battery energy storage system model is at the utility-scale level and operated using a four-quadrant control mode. The battery energy storage system topology is a three-phase universal topology. Figure 3 shows the block diagram of the model. The battery energy storage system model consists of the renewable energy plant control (REPC_A) model, the renewable energy electrical control (REEC_C) model, and the renewable energy generator/converter control (REGC_A) model.

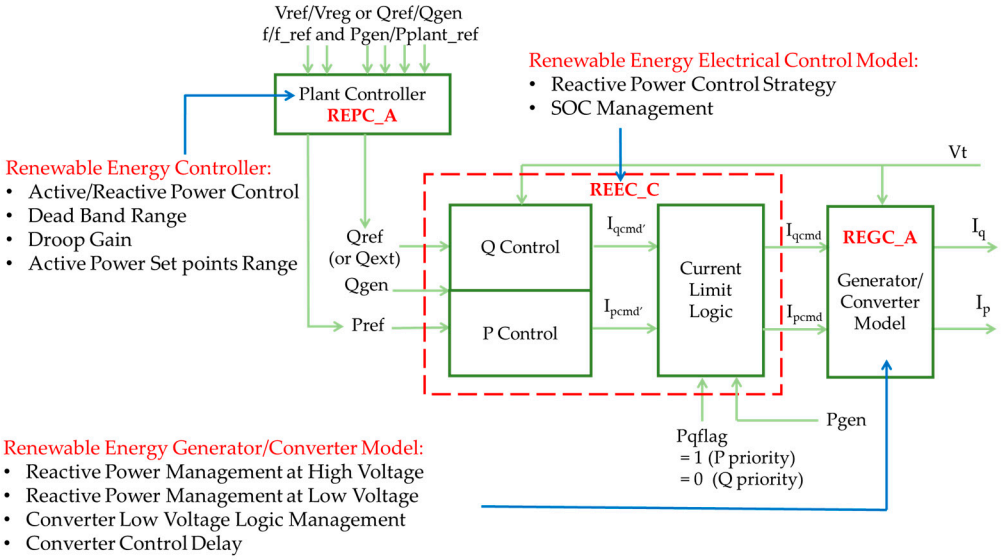


Figure 3. The block diagram of the battery energy storage system [26].

The control block diagram of the REPC_A model includes the active power control block and the reactive power control block. The important parameters of the active power control block of the REPC_A model include the deadband range, droop gain, PI controller settings, and command value range settings. Figure 4 depicts the control block diagram of the REPC_A model.

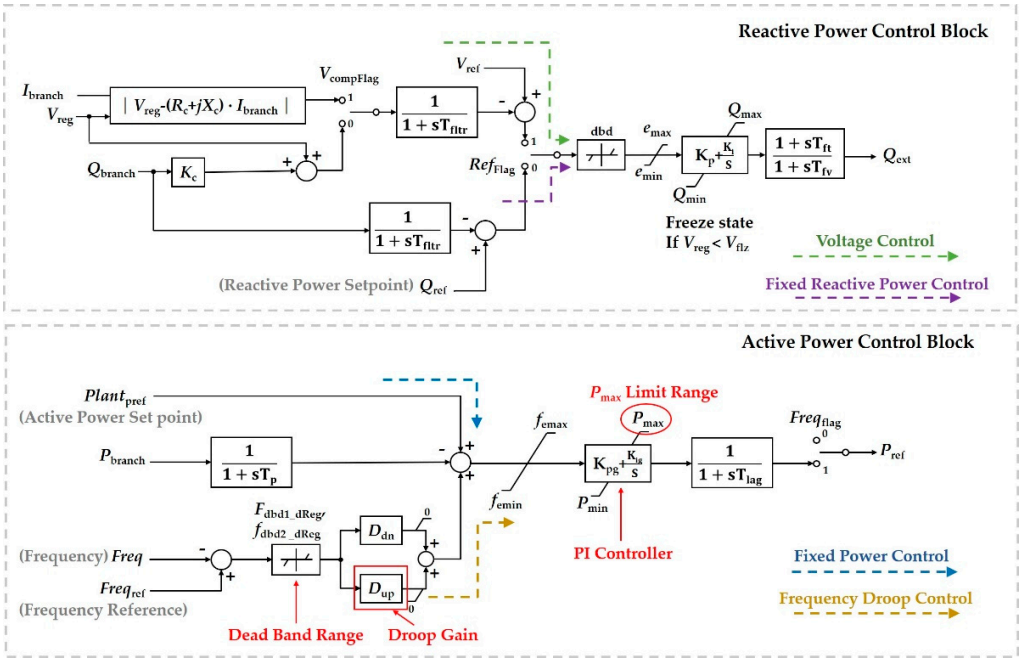


Figure 4. The block diagram of the REPC_A model [27,28].

The control block diagram model of the REEC_C model includes the active power control block and reactive power control block. The important parameter in the active power control block is the protection and determination of the state of charge (SOC). The reactive power control block utilizes flag selection to adjust different functions. As shown in Figure 5, it represents the control block diagram model of the REEC_C model.

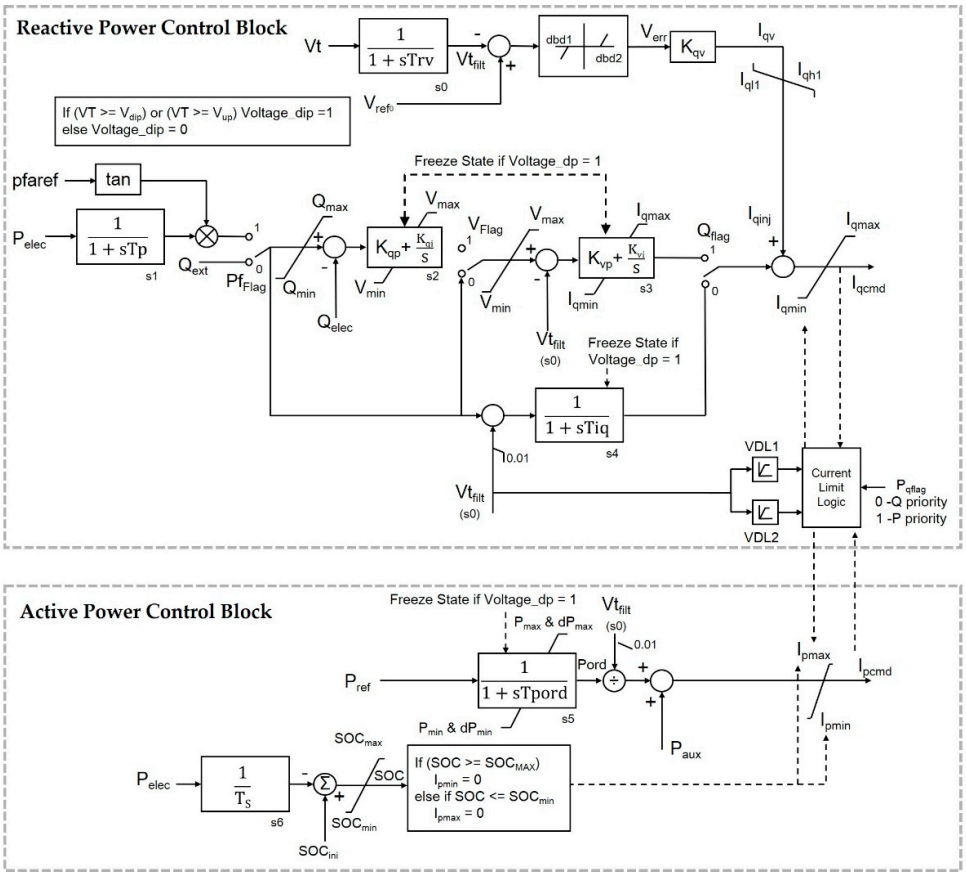


Figure 5. The block diagram of the REEC_C model [29].

The control block diagram model of the REGC_A model: This model primarily includes converter response time constants, low-voltage logic management, low-voltage active power management, and high-voltage reactive power management. The converter response time constants are used to adjust the response speed of the converter. Low-voltage logic management is employed to control the behavior of the converter under low-voltage conditions. Low-voltage active power management prevents low voltage by regulating active power. High-voltage reactive power management prevents overvoltage by regulating reactive power. As shown in Figure 6, it represents the control block diagram model of the REGC_A model.

3.1. Static Regulation Control Model

The static regulation control model needs to consider frequency precision, triggering conditions, deadband range, and response speed. Setting these control parameters accurately is essential for ensuring the effective operation of the static regulation control system. Therefore, for the static regulation control model based on the WECC second-generation generic model, and the corresponding control parameters must be designed. When the static regulation strategy is not active, the upper threshold of the static regulation control model is 59.88 Hz. The symbol of the upper threshold is f_{dbd2}, and the calculation equation can be written as follows:

$$f_{dbd2_sReg} = \frac{-59.88 + 60}{60} = 0.002 \text{ pu} \quad (1)$$

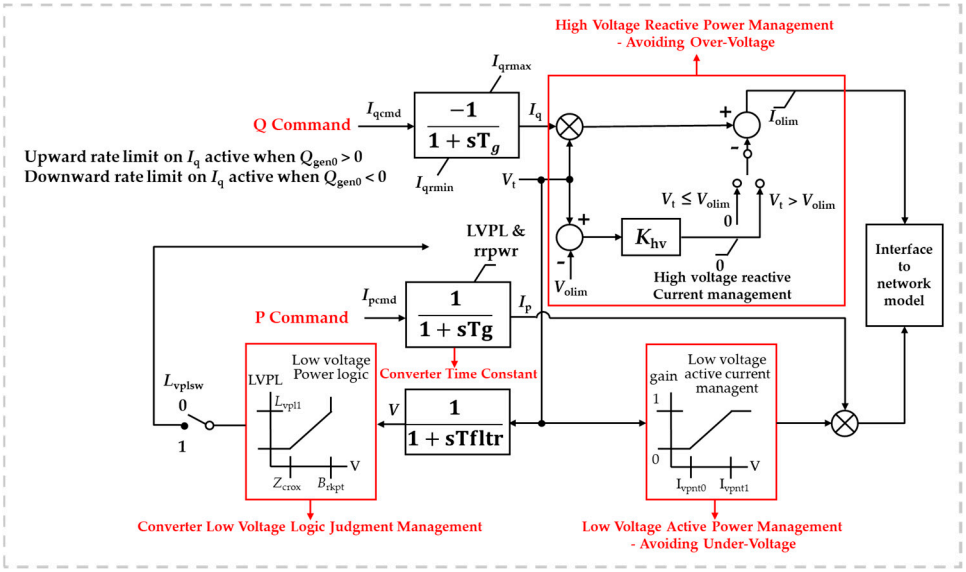


Figure 6. The block diagram of the REGC_A model [27,28].

When the static regulation strategy is active, the upper threshold of the static regulation control model is 59.98 Hz. The symbol of the upper threshold is $f_{dbd2'_sReg}$, and the calculation equation can be written as follows:

$$f_{dbd2'_sReg} = \frac{-59.98+60}{60} = 0.00033333 \text{ pu} \quad (2)$$

Here, we assume that the flexible adjustment range of the static regulation control model is not considered. The lower threshold of the static regulation control model is 60 Hz, and the symbol of the lower threshold is f_{dbd1}, and its value is designed to be 0. The frequency detection precision of the battery storage system is $\pm$0.001 Hz. When the grid frequency touches the upper threshold, f_{dbd2}, and the grid frequency is $\leq$59.879 Hz, the battery energy storage system outputs an active power command, which is 1 pu. Therefore, the function of the droop gain, D_{up_sReg}, can be written as follows:

$$D_{up_sReg} \geq \frac{P_{start} - P_0}{-f_{start} + f_{ref} - f_{dbd2}} \quad (3)$$

Equations (1)–(3) are defined as follows:

D_{up_sReg}, under frequency droop gain of static regulation control model (pu);
P_{start}, starting output power value (pu);
P_0, initial output power value (pu);
f_{start}, starting output frequency value (pu);
f_{ref}, grid frequency reference value (pu);
f_{dbd2_sReg}, upper frequency threshold of static regulation control model (pu);
$f_{dbd2'_sReg}$, upper frequency threshold of static regulation control model under strategy operation (pu).

According to the proposed static regulation control model, the frequency detection accuracy and upper threshold are considered. The droop gain of the static regulation control model is designed to be 60,000.

3.2. Dynamic Regulation Control Model

The characteristics of the dynamic regulation control model are generally divided into the frequency detection, deadband range, frequency operating range, and droop gain of active power. For the dynamic regulation control model based on the WECC second-

generation generic model, the corresponding parameters must be designed. Assuming that the flexible adjustment range is not considered, the frequency of the upper threshold is designed at 59.98 Hz. The symbol of the upper threshold is f_{dbd2_dReg}, and the calculation equation can be written as follows:

$$f_{dbd2_dReg} = \frac{-59.98 + 60}{60} = 0.00033333 \text{ pu} \quad (4)$$

If the lower threshold of the dynamic regulation control model is set at 60.02 Hz, the symbol of the lower threshold is f_{dbd1_dReg}, and the calculation equation can be written as follows:

$$f_{dbd1_dReg} = \frac{-60.02 + 60}{60} = -0.00033333 \text{ pu} \quad (5)$$

When the grid frequency is less than 59.98 Hz, the battery energy storage system will provide active power to the grid based on the droop gain. The under frequency of droop gain function can be written as follows:

$$D_{up_dReg} = \frac{P_{max} - P_0}{-f_{max} + f_{ref} - f_{dbd2_dReg}} \quad (6)$$

When the grid frequency is greater than 60.02 Hz, the battery energy storage system will charge active power from the grid based on the droop gain. The over frequency of droop gain function can be written as follows:

$$D_{dn_dReg} = \frac{P_{max} - P_0}{-f_{min} + f_{ref} - f_{dbd1_dReg}} \quad (7)$$

Equations (6) and (7) are defined as follows:

D_{up_dReg}, under frequency droop gain of the dynamic regulation control model (pu);
D_{dn_dReg}, over frequency droop gain of the dynamic regulation control model (pu);
P_{max}, maximum output power value (pu);
P_0, initial output power value (pu);
f_{max}, maximum under frequency value (pu);
f_{min}, minimum over frequency value (pu);
f_{ref}, grid frequency value (pu);
f_{dbd2_dReg}, upper threshold of the dynamic regulation control model (pu);
f_{dbd1_dReg}, lower threshold of the dynamic regulation control model (pu).

Therefore, based on the proposed dynamic regulation control model, the droop gains of under frequency and over frequency for dReg 0.25 and dReg 0.5 are 260.8696 and 125, respectively.

3.3. Virtual Inertia Control Model

The WECC second-generation generic model is not able to make detailed changes to the hardware and control methods, such as the switch switching methods and component values. To address this, a swing equation emulation for virtual inertial control is adopted. Next, the theory of virtual inertia control model is introduced in this section.

A generator converts mechanical energy into electrical energy by cutting through magnetic lines of force with the rotation of its rotor. This means that, when there is an object with mass and rotational speed, the object generates kinetic energy. The equation for the rotational kinetic energy contained in a virtual rotating mass with rotational inertia can be written as follows:

$$E = \frac{1}{2} J \omega^2 \quad (8)$$

The mechanical power of a virtual rotating mass is the time derivative of kinetic energy, and both the angular frequency and rotational inertia are functions of time. The equation for the mechanical power of a virtual rotating mass can be written as follows:

$$P_{mech} = \frac{1}{2}\omega(t)^2 \frac{d}{dt}J(t) + J(t)\omega(t)\frac{d}{dt}\omega(t) \tag{9}$$

To simplify the analysis, let us assume that the rotational inertia of the virtual mass is constant, and the angular velocity of the virtual rotating mass is equal to the grid's angular velocity, which is at its rated value [24]. The simplified dynamic equation for the swing equation emulation can be written as follows:

$$P_{mech} = J\omega_{grid}\frac{d}{dt}\omega_{grid}(t) \tag{10}$$

Equations (8)–(10) are defined as follows:

E, kinetic energy of virtual rotating mass (J);
J, rotational inertia of virtual mass (kg·m^2);
ω, angular velocity of virtual mass (rad/s);
P_{mech}, mechanical power of virtual rotating mass (W);
ω_{grid}, rated angular velocity of the power system (rad/s);
$\frac{d}{dt}\omega_{grid}(t)$, rate of change of angular velocity of the power system.

The equation for the inertia constant, H, can be written as Equation (11). By combining Equation (10) with Equation (11), the dynamic swing equation with the inertia constant can be written as follows:

$$H = \frac{J{\omega_{grid}}^2}{2S_B} \tag{11}$$

$$P_{mech} = \frac{2HS_B}{\omega_{grid}}\frac{d}{dt}\omega_{grid}(t) \tag{12}$$

Equations (11) and (12) are defined as follows: H, inertia constant (s); and S_B, capacity of a battery energy storage system (VA).

The mechanical power is written per unit, and the grid frequency parameter is used instead of the angular velocity parameter. The dynamic swing equation per unit can be written as follows:

$$P_{mech(pu)} = \frac{P_{mech}}{S_B} = \frac{2H}{f_{grid}}\frac{d}{dt}f_{grid}(t) \tag{13}$$

We assume that the output power of the battery energy storage system is a positive value, which means that the output power is injected into the grid. The relationship between the mechanical power equation of the virtual rotating mass and the output power of the battery energy storage system can be written as follows:

$$P_{BESS(pu)} = -P_{mech(pu)} = -\frac{2H}{f_{grid}}\frac{d}{dt}f_{grid}(t) \tag{14}$$

Equations (13) and (14) are defined as follows:

P_{mech}(pu), mechanical power of virtual rotating mass per unit (pu);
f_{grid}, rated frequency of power system;
$\frac{d}{dt}f_{grid}$(t), rate of change of frequency of power system;
P_{BESS}(pu), output power of battery energy storage system per unit (pu).

4. Frequency Regulation Technology Simulation

4.1. Scenario Assumption

In this paper, the PSS/E v34 software is used to verify the proposed control model. The Taiwan 2025 power system condition is used to perform the simulation. In the simulation, the devices of generation, transformer, and transmission are actual device parameters. The load parameters are amplified based on historical load parameters, and the status of power generation is the result of the economic dispatch. The installed renewable energy installed capacity in the Taiwan 2025 power system is expected to be 26.938 GW. The scenario assumptions are shown in Table 4. The hourly maximum generation of solar power capacity is 90% during summer, and the hourly maximum generation of solar power capacity is 70% during winter. The distributions of solar power are as follows: 5% in the north region, 35% in the central region, and 60% in the south region.

Table 4. The parameters of scenario assumptions.

Scenario	2025 Light Load	2025 Peak Load
Load (MW)	21,104	39,818.7
Renewable energy installed Capacity (MW)	26,938 (Solar power: 20,000; wind power: 6938)	
Hourly maximum generation (MW)	14,000	18,000

Because the effectiveness of the proposed strategies needs to be evaluated, the most serious N-1 events are designed. The total capacity of the tripped generation unit is 1271.4 MW. Continuing, in order to make the response of the battery energy storage system model close to the response of the actual device, the response parameters of the battery energy storage system are based on the Delta's PCS 100 model. Therefore, the battery energy storage system is installed on the 161 kV in Taipei, Taiwan. Therefore, the generation status, load level, renewable energy capacity, hourly maximum generation of solar power, device distribution, and response of battery energy storage systems are considered in the scenario assumptions. Additionally, the WECC second-generation battery energy storage system model does not provide a control module for the proposed virtual inertia control model. This paper formulates a dynamic swing equation of the proposed virtual inertia control model using an external programming language. The rise time and delay time are designed in the WECC second-generation generic model. Therefore, the external programming language is combined with the WECC second-generation generic model constitutes the proposed virtual inertia control model.

4.2. Simulation of Light Load Scenario

Based on the same assumptions for the light load scenario, simulations are operated using different control methods for the battery energy storage system. Figure 7 shows the comparative graphs of the grid frequency and battery energy storage system output power for the 2025 light load scenario. The simulation results for the proposed strategies are presented in Table 5. Without frequency regulation from the battery energy storage system, the frequency nadir for this scenario is 59.270 Hz. With frequency regulation control using dReg0.5 and dReg0.25, the frequency nadir values are 59.625 Hz and 59.730 Hz, respectively. When the static regulation is operated by the battery energy storage system, and the response time of output power is 353 ms, the frequency nadir for this scenario is 59.766 Hz. The virtual inertia control of the inertia constant parameter is 12, and the frequency nadir is 59.312 Hz.

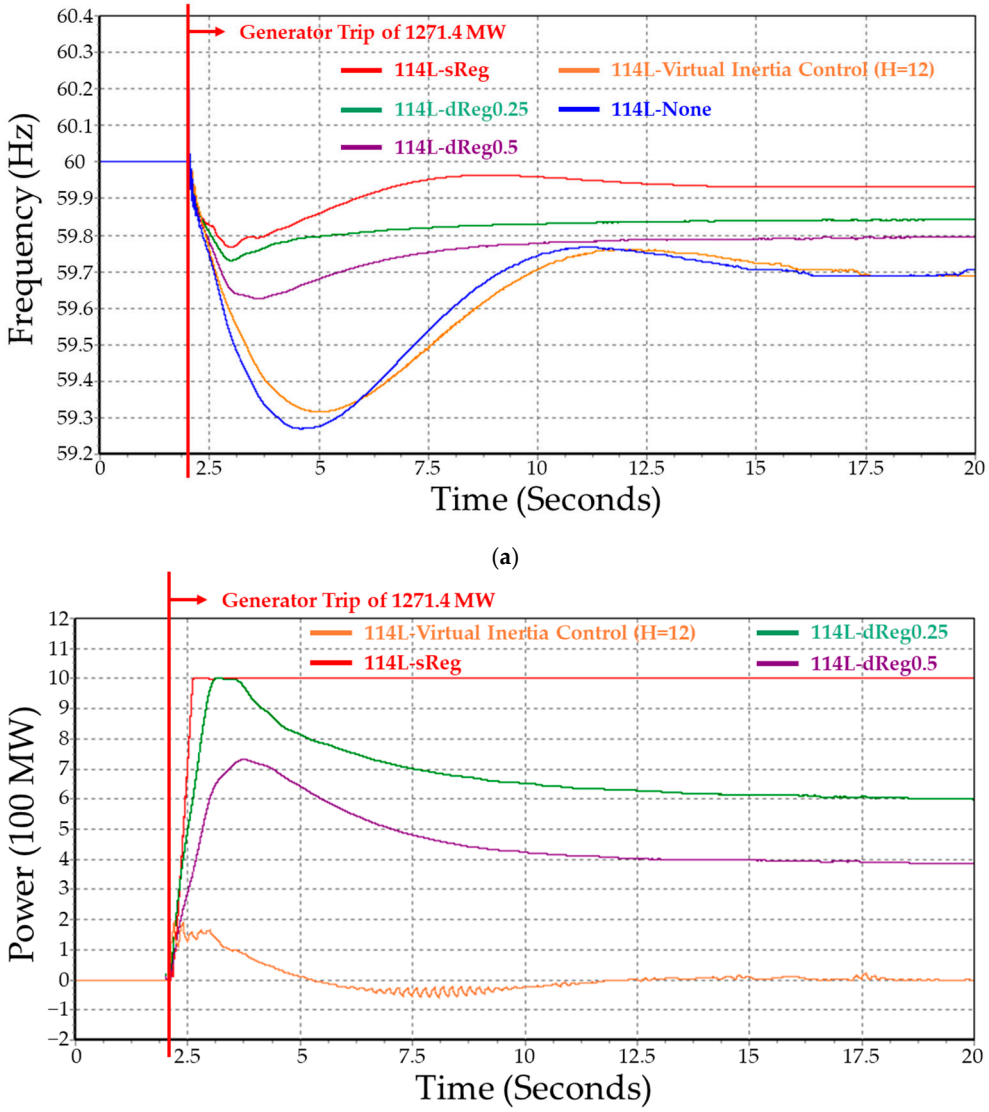


Figure 7. Simulations for 2025 light load scenario: (**a**) grid frequencies and (**b**) battery energy storage system power output.

Table 5. Simulations of grid frequency for 2025 light load scenario.

Strategy Name	Frequency Nadir (Hz)	Deviation (Hz)
None	59.270	0
dReg 0.5	59.625	0.355
dReg 0.25	59.730	0.460
sReg	59.766	0.496
Virtual inertia Control @ H = 12	59.312	0.042

4.3. Simulation of Peak Load Scenario

According to the peak load scenario assumption, the proposed strategies are operated under the battery energy storage system. The comparison of the grid frequency and battery energy storage system output power for the 2025 peak load scenario is shown in Figure 8. The simulation results for the proposed strategies are shown in Table 6. Without frequency regulation for battery energy storage systems, the frequency nadir is 59.588 Hz. When the battery energy storage system is operated with frequency regulation control of dReg0.5

and dReg0.25, the frequency nadir of simulation results are 59.726 Hz and 59.789 Hz, respectively. The frequency nadir with static regulation is 59.868 Hz, and the rise time of the output power is 367 ms. When the grid frequency recovers to 59.98 Hz, the battery energy storage system rapidly reduces its compensating power, causing the system frequency to drop again. Subsequently, as the grid frequency falls to 59.88 Hz, the battery energy storage system triggers the upper threshold of static regulation control once more. This situation causes frequency oscillations in the grid during the frequency recovery period. The virtual inertia control of the inertia constant parameter is 40, and the frequency nadir is 59.633 Hz.

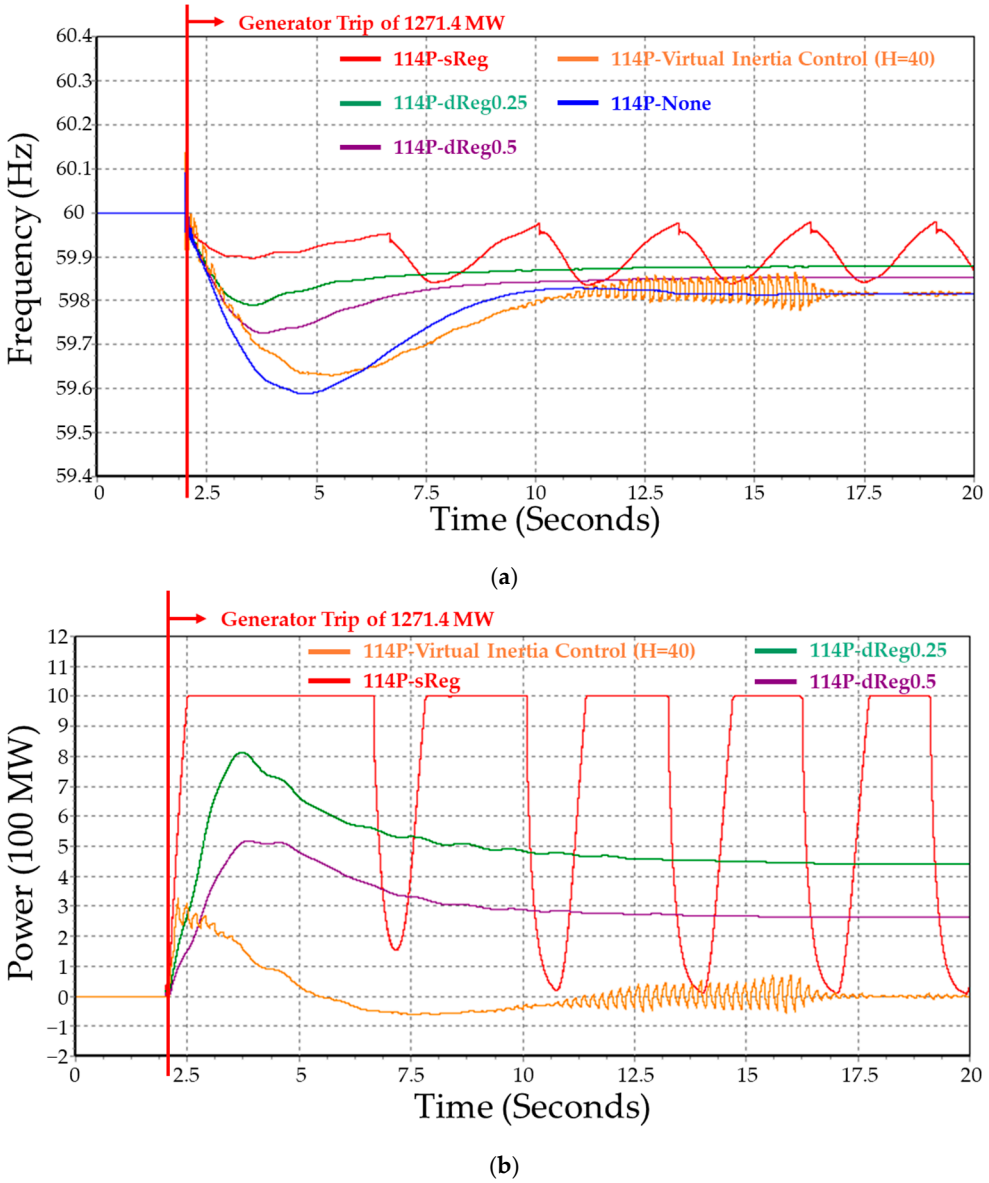


Figure 8. Simulations for 2025 peak load scenario: (**a**) grid frequencies and (**b**) battery energy storage system power output.

Table 6. Simulations of grid frequency for 2025 peak load scenario.

Strategy Name	Frequency Nadir (Hz)	Deviation (Hz)
None	59.588	0
dReg 0.5	59.726	0.138
dReg 0.25	59.789	0.201
sReg	59.868	0.280
Virtual inertia Control @ H = 40	59.633	0.045

4.4. Analysis of Frequency Regulation Technologies

This paper discusses the evaluation of proposed strategies based on the simulation results. The comparison factors of the strategies include the RoCoF, frequency nadirs, frequency recovery, and system oscillation regulation. The capability of limiting the RoCoF is evaluated using the output power of the battery energy storage system when the fault occurs. The capability to mitigate frequency nadirs is evaluated based on the simulation results of N-1 events. The capability of frequency recovery is determined by the interval of the grid frequency nadir to the steady-state frequency. The capability of the system oscillation regulation is determined by the frequency regulation before a fault occurs. According to the simulation results of the light load scenario, the biggest frequency deviation is 0.496 Hz. The sReg strategy is best among RoCoF limitations. The simulation results of the steady-state frequency and energy of battery energy storage systems are shown in Table 7. The inertia energy is defined as the output power that the battery energy storage system provides in the 0.2 s after the N-1 event occurs.

Table 7. The simulation results of steady-state frequency and energy of the battery energy storage system.

Strategy Name	Light Load Scenario		Peak Load Scenario	
	Energy (MJ)	Steady-State Frequency (Hz)	Energy (MJ)	Steady-State Frequency (Hz)
None	-	59.705	-	59.816
dReg 0.5	4.73	59.794	3.52	59.853
dReg 0.25	7.92	59.841	6.00	59.878
sReg	2.23	59.868	25.83	-
Virtual inertia Control	13.40	59.687	10.73	59.815

In the light load scenario, the energy of the battery energy storage system under the virtual inertia strategy is 13.40 MJ. In the peak load scenario, the energy of the battery energy storage system under the virtual inertia strategy is 10.73 MJ. The energy of the battery energy storage system under static regulation strategy is maximum at 25.83 MJ for the peak load scenario. Therefore, the virtual inertia strategy and the static regulation strategy have a better limiting capability for RoCoF compared to dReg 0.25 and dReg 0.5. In the light load scenario, the steady-state frequency under the static regulation strategy is 59.868 Hz, and the steady-state frequency under the dReg 0.25 strategy is 59.841 Hz. In the peak load scenario, the steady-state frequency under the dReg 0.25 strategy is 59.878 Hz, and the grid frequency under the static regulation strategy is not in the steady state. However, the steady-state frequency under the virtual inertia strategy decreases compared to the steady-state frequency without any strategy. The capability of system oscillation regulation is determined by the frequency of the deadband range. Before the fault occurs, the RoCoF is small, indicating that the output power of the virtual inertia strategy is small. The dReg 0.25 and dReg 0.5 strategies have droop gain, so the capability of the system oscillation under the dReg strategy is better than it is under the other strategies. A comparison of the proposed strategies under the battery energy storage system is shown in Table 8.

Table 8. Comparison of battery energy storage system regulation technology capability.

Name	RoCoF Limitation	Frequency Nadir	Frequency Recovery	System Oscillation Regulation
dReg 0.5	Weak	Strong	Medium	Strong
dReg 0.25	Medium	Strong	Medium	Strong
sReg	Strong	Strong	Weak	Weak
Virtual Inertia control	Strong	Medium	Weak	Medium

According to the proposed analysis results, the dynamic regulation strategy has good capability in regard to frequency nadir and frequency recovery, but its capability regarding RoCoF limitation is weak when the parameter is set to 0.5. The static regulation strategy has good capability regarding frequency nadir, and its capability regarding RoCoF limitation is great when the power system has a peak load. However, when the battery energy storage system with a large capacity operates according to the static regulation strategy, the grid frequency will oscillate during the frequency recovery period. Additionally, the static regulation strategy has weak capability in regard to system oscillation regulation because the strategy of the frequency deadband is larger than that of other strategies. The virtual inertia strategy has good capability regarding RoCoF limitation, and the capability of RoCoF limitation can be maintained under light load and peak load. However, its frequency recovery capability is weak because the battery energy storage is in the charging state during this period. Therefore, the improvements that need to be made to the strategy are as follows:

1. Static regulation strategy: When the power system has a peak load and larger battery energy storage system capacity, the recovery time of compensation needs to be limited under the static regulation strategy. The problem of frequency oscillation can be avoided during the frequency recovery period.
2. Virtual inertia control: The virtual inertia strategy can be directly replaced by the dynamic regulation strategy when the battery energy storage system is operating in the charging state. The weak capability of frequency recovery can be strengthened by the combination of strategies.

Finally, according to the analysis results, the capability evaluation and improvement points of the strategy lay the foundation for large-capacity battery energy storage systems. It can help power operators design the battery energy storage operation strategy, when the system is peak load or light load, and it can help them avoid designing the wrong strategy to support the power system. At the same time, correct strategies can be implemented for the weak capabilities of the power system to achieve the best benefits of the strategy. In addition, the proposed strategy improvement suggestions can help improve the capability of the battery energy storage system operating strategy.

5. Conclusions

Battery energy storage systems play a crucial role in the future new power system structure, contributing to the resilience and stability of the power system under various control methods. This paper analyzes three strategies, which are static regulation, dynamic regulation, and swing equation emulated by virtual inertia control. The strategies model based on the WECC second-generation generic model to design, and the battery energy storage model under three strategies consider the factors of frequency response, which include the frequency detection, deadband range, frequency operating range, and droop gain. Additionally, this paper uses the external programming language combined with the WECC second-generation generic model to reach the virtual inertial strategy. The simulation condition is used in the Taiwan 2025 power system condition, which is considered the actual device. The devices include generators, power transformers, renewable energy

generators, the battery energy storage system, the transmission line, and the load. The condition factors include generation statutes, renewable generation distribution, N-1 event level, load size, and output power response of battery energy storage systems.

According to the N-1 event of simulation results, the capability of three strategies is analyzed. The evaluation focuses on the capabilities of RoCoF limitation, frequency nadir, frequency recovery, and system oscillation regulation. In the light load, the battery storage system operates under the static regulation strategy, and the deviation of the frequency nadir compared with the dReg0.50, dReg0.25, and virtual inertial control is increased by 1.08 times, 1.4 times, and 11.81 times, respectively. The battery storage system operates according to a virtual inertial strategy; the energy of the battery energy storage of the dReg0.50, dReg0.25, and static regulation increases by 2.83 times, 1.69 times, and 6.01 times. The battery storage system operates according to the dReg 0.25 strategy, and the deviation of the steady-state frequency compared with the dReg0.50 and static regulation increases by 1.53 times, 0.83 times, and 11.81 times, respectively. The deviation of the steady-state frequency of the virtual inertial strategy is a negative value. However, when the large battery storage system operates under the static regulation strategy, the grid frequency oscillates during the frequency recovery period. Therefore, the dynamic regulation strategy shows good capability in regard to frequency nadir and frequency recovery. The static regulation strategy shows good capability in regard to frequency nadir, and the capability of the RoCoF limitation is better when it is used in the peak load. In the peak load and light load, the virtual inertia strategy shows the good capability in regard to the RoCoF limitation. According to the analysis results, the static regulation strategy needs to limit the recovery time of the battery storage system, and the virtual inertia strategy can be directly replaced by the dynamic regulation strategy when the battery energy storage system is operating in the charging state. Finally, the proposed strategy models and the analysis results can help power operators to design the battery energy storage operation strategy when the system is peak load or light load, and it can help designers avoid designing the wrong strategy to support the power system.

In addition, the future works proposed by this paper are as follows: First, the battery energy storage system model added factors such as communication delays. Continuing, the economic factors of battery energy storage systems for frequency regulation technologies are analyzed, the factors include capital costs, maintenance costs, and potential revenue streams. Finally, the proposed frequency regulation technology will be added to the stacking services. There should be a combination with the energy regulation technology, which is peak shaving and valley filling or virtual power line technology. The economic benefits of battery storage systems can be increased.

Author Contributions: Conceptualization, L.-Y.L., W.-C.C., T.-Y.C. and C.-C.K.; methodology, L.-Y.L.; software, L.-Y.L.; validation, L.-Y.L., W.-C.C. and C.-C.K.; formal analysis, L.-Y.L., W.-C.C., T.-Y.C. and C.-C.K.; investigation, L.-Y.L. and C.-C.K.; resources, L.-Y.L. and C.-C.K.; data curation, L.-Y.L., W.-C.C. and C.-C.K.; writing—original draft preparation, L.-Y.L.; writing—review and editing, C.-C.K. All authors have read and agreed to the published version of the manuscript.

Funding: This research received no external funding.

Institutional Review Board Statement: Not applicable.

Informed Consent Statement: Not applicable.

Data Availability Statement: All data is already provided in this article.

Acknowledgments: Support for this research from Institute of Power Systems, Taiwan Power Company, is gratefully acknowledged.

Conflicts of Interest: The authors declare no conflict of interest.

Nomenclature

sReg	the steady regulation
REPC	the renewable energy plant control
REGC	the renewable energy generator/converter control
BESS	the battery energy storage system
D_{up_sReg}	the under-frequency droop gain of static regulation control model
P_0	the initial output power value
f_{ref}	the grid frequency reference value
$f_{dbd2'_sReg}$	the upper-frequency threshold of static regulation control model under strategy operation
D_{dn_dReg}	the over-frequency droop gain of dynamic regulation control model
f_{max}	the maximum under frequency value
f_{ref}	the grid frequency value
f_{dbd1_dReg}	the lower threshold of dynamic regulation control model
J	the rotational inertia of the virtual mass
P_{mech}	the mechanical power of the virtual rotating mass
$\frac{d}{dt}\omega_{grid}$	the rate of change of angular velocity of the power system
S_B	the capacity of a battery energy storage system
f_{grid}	the rated frequency of the power system
$P_{BESS(pu)}$	the output power of battery energy storage system per unit
dReg	the dynamic regulation
REEC	the renewable energy electrical generator control
RoCoF	the rate of change of frequency
SOC	the state of charge
P_{start}	the starting output power value
f_{start}	the starting output frequency value
f_{dbd2_sReg}	the upper-frequency threshold of static regulation control model
D_{up_dReg}	the under-frequency droop gain of dynamic regulation control model
P_{max}	the maximum output power value
f_{min}	the minimum over frequency value
f_{dbd2_dReg}	the upper threshold of dynamic regulation control model
E	the kinetic energy of the virtual rotating mass
ω	the angular velocity of the virtual mass
ω_{grid}	the rated angular velocity of the power system
H	the inertia constant
$P_{mech(pu)}$	the mechanical power of virtual rotating mass per unit
$\frac{d}{dt}f_{grid}$	the rate of change of frequency of the power system

References

1. Kassem, Y.; Abdalla, M.H.A. Modeling predictive suitability to identify the potential of wind and solar energy as a driver of sustainable development in the Red Sea State, Sudan. *Environ. Sci. Pollut. Res.* **2022**, *29*, 44233–44254. [CrossRef] [PubMed]
2. Ndirangu, J.; Nderu, J.; Irungu, G. Impact of Variation of Virtual Inertia and Virtual Damping on Frequency and Power Angle Responses of Virtual Inertia Emulation Controlled Converter. In Proceedings of the IEEE PES/IAS PowerAfrica, Kigali, Rwanda, 22–26 August 2022; pp. 1–4. [CrossRef]
3. Julius, N.; Nderu, J.N.; Irungu, G.K. Frequency Control and Virtual Inertia Emulation Techniques for Grid Connected Wind Energy Conversion Systems—A Review. In Proceedings of the 2019 IEEE AFRICON, Accra, Ghana, 25–27 September 2019; pp. 1–6. [CrossRef]
4. Fernández-Guillamón, A.; Gómez-Lázaro, E.; Muljadi, E.; Molinagarcía, Á. Power systems with high renewable energy sources: A review of inertia and frequency control strategies over time. *Renew. Sustain. Energy Rev.* **2019**, *115*, 109369. [CrossRef]
5. Akbari, M.A.; Aghaei, J.; Barani, M.; Savaghebi, M.; Shafie-Khah, M.; Guerrero, J.M.; Catalao, J.P. New Metrics for Evaluating Technical Benefits and Risks of DGs Increasing Penetration. *IEEE Trans. Smart Grid* **2017**, *8*, 2890–2902. [CrossRef]
6. Kim, J.; Muljadi, E.; Park, J.W.; Kang, Y.C. Adaptive Hierarchical Voltage Control of a DFIG-Based Wind Power Plant for a Grid Fault. *IEEE Trans. Smart Grid* **2016**, *7*, 2980–2990. [CrossRef]
7. Abreu, T.; Soares, T.; Carvalho, L.; Morais, H.; Simão, T.; Louro, M. Reactive Power Management Considering Stochastic Optimization under the Portuguese Reactive Power Policy Applied to DER in Distribution Networks. *Energies* **2019**, *12*, 4028. [CrossRef]
8. Yang, Z.; Han, J.; Li, L.; Deng, Y.; Yang, F.; Lei, Y.; Min, H.; Hu, W.; Su, L. Research of Islanding Operation and Fault Recovery Strategies of Distribution Network Considering Uncertainty of New Energy. *Electronics* **2023**, *12*, 4230. [CrossRef]

9. Fang, C.; Tang, Y.; Ye, R.; Lin, Z.; Zhu, Z.; Wen, B.; Ye, C. Adaptive Control Strategy of Energy Storage System Participating in Primary Frequency Regulation. *Processes* **2020**, *8*, 687. [CrossRef]
10. McMahon, J.; Kërçi, T.; Milano, F. Combining Flexible Loads with Energy Storage Systems to provide Frequency Control. In Proceedings of the IEEE PES Innovative Smart Grid Technologies—Asia (ISGT Asia), Brisbane, Australia, 5–8 December 2021; pp. 1–5. [CrossRef]
11. Atif, A.; Khalid, M.; Leber, G. Saviztky–Golay Filtering for Solar Power Smoothing and Ramp Rate Reduction Based on Controlled Battery Energy Storage. *IEEE Access* **2020**, *8*, 33806–33817. [CrossRef]
12. Gusev, Y.P.; Subbotin, P.V. Using Battery Energy Storage Systems for Load Balancing and Reactive Power Compensation in Distribution Grids. In Proceedings of the International Conference on Industrial Engineering, Applications and Manufacturing (ICIEAM), Sochi, Russia, 25–29 March 2019; pp. 1–5. [CrossRef]
13. Ma, C.; Sun, J.; Huang, J.; Wang, K. Transient Stability Enhancement Strategy for Islanded Microgrids Based on Energy Storage–Virtual Synchronous Machine Control. *Energies* **2023**, *16*, 6390. [CrossRef]
14. Gouveia, J.; Moreira, C.L.; Peças Lopes, J.A. Improving Dynamic Security in Islanded Power Systems: Quantification of Minimum Synchronous Inertia Considering Fault-Induced Frequency Deviations. *Electricity* **2023**, *4*, 114–133. [CrossRef]
15. Li, S.; Xu, Q.; Huang, J. Research on the integrated application of battery energy storage systems in grid peak and frequency regulation. *J. Energy Storage* **2023**, *59*, 106459. [CrossRef]
16. Vargas, L.S.; Bustos-Turu, G.; Larraín, F. Wind Power Curtailment and Energy Storage in Transmission Congestion Management Considering Power Plants Ramp Rates. *IEEE Trans. Power Syst.* **2015**, *30*, 498–2506. [CrossRef]
17. Zhu, Y.; Zang, H.; Cheng, L.; Gao, S. Output Power Smoothing Control for a Wind Farm Based on the Allocation of Wind Turbines. *Appl. Sci.* **2018**, *8*, 980. [CrossRef]
18. Kim, H.; Lee, J.; Lee, J.; Jang, G. Novel Coordinated Control Strategy of BESS and PMSG-WTG for Fast Frequency Response. *Appl. Sci.* **2021**, *11*, 3874. [CrossRef]
19. Malozyomov, B.V.; Martyushev, N.V.; Voitovich, E.V.; Kononenko, R.V.; Konyukhov, V.Y.; Tynchenko, V.; Kukartsev, V.A.; Tynchenko, Y.A. Designing the Optimal Configuration of a Small Power System for Autonomous Power Supply of Weather Station Equipment. *Energies* **2023**, *16*, 5046. [CrossRef]
20. Malozyomov, B.V.; Martyushev, N.V.; Sorokova, S.N.; Efremenkov, E.A.; Qi, M. Mathematical Modeling of Mechanical Forces and Power Balance in Electromechanical Energy Converter. *Mathematics* **2023**, *11*, 2394. [CrossRef]
21. Taiwan Electric Power Company. *Power Trading Platform Management Specifications, Operating Procedures Revised General Instructions and Comparison Table*; Taiwan Electric Power Company: Taipei City, Taiwan, 2023.
22. Beck, H.-P.; Hesse, R. Virtual synchronous generators. In Proceedings of the 9th International Conference of Electrical Power Quality and Utilisation, Barcelona, Spain, 9–11 October 2007; pp. 1–6. [CrossRef]
23. Driesen, J.; Visscher, K. Virtual synchronous generators. In Proceedings of the IEEE Power and Energy Society General Meeting—Conversion and Delivery of Electrical Energy in the 21st Century, Pittsburgh, PA, USA, 20–24 July 2008; pp. 1–3. [CrossRef]
24. Visscher, K.; De Haan, S.W.H. Virtual synchronous machines (VSG's) for frequency stabilisation in future grids with a significant share of decentralized generation. In Proceedings of the CIRED Seminar 2008: SmartGrids for Distribution, Frankfurt, Germany, 23–24 June 2008; pp. 1–4.
25. Zhong, Q.-C.; Weiss, G. Synchronverters: Inverters That Mimic Synchronous Generators. *IEEE Trans. Ind. Electron.* **2011**, *58*, 1259–1267. [CrossRef]
26. Western Electricity Coordinating Council Modeling and Validation Work Group. *WECC Battery Storage Dynamic Modeling Guideline*; Western Electricity Coordinating Council: Salt Lake City, UT, USA, 2016.
27. EPRI. *Model User Guide for Generic Renewable Energy System Models*; Electric Power Research Institute: Palo Alto, CA, USA, 2015.
28. Xu, X.; Bishop, M.; Oikarinen, D.G.; Hao, C. Application and modeling of battery energy storage in power systems. *CSEE J. Power Energy Syst.* **2016**, *2*, 82–90. [CrossRef]
29. Siemens Industry. *Model Library*; PSSE 34.6.1.; Siemens: Munich, Germany, 2019.

Disclaimer/Publisher's Note: The statements, opinions and data contained in all publications are solely those of the individual author(s) and contributor(s) and not of MDPI and/or the editor(s). MDPI and/or the editor(s) disclaim responsibility for any injury to people or property resulting from any ideas, methods, instructions or products referred to in the content.